

# Evaluating the Corrosion Level of Bare Steel Bars with Pitting Corrosion by DOFS

S.S. Zhang<sup>1</sup>, Y.X. Li<sup>1</sup>, E Chen<sup>1</sup>

<sup>1</sup> School of Civil and Hydraulic Engineering, Huazhong University of Science and Technology, Wuhan, China, [chene@hust.edu.cn](mailto:chene@hust.edu.cn) (Corresponding author)

**Abstract.** *Steel corrosion is one of the main causes of the deterioration of reinforced concrete structures. Localized pitting corrosion of rebar is particularly harmful, as it can severely damage mechanical properties of steel rebar including both the load and deformation capacities. Moreover, unlike uniform corrosion which can give a warning by causing extensive longitudinal cracking, pitting corrosion is often more hidden with the absence of obvious corrosion cracks. Traditional non-destructive methods based on electrochemistry may encounter large errors when estimating the pitting corrosion level in concrete; as a result, more effective methods/tools are in necessity for a timely and accurate detection of localized pitting corrosion. This study investigates the ability of distributed optical fiber sensors (DOFS) to measure pitting corrosion of steel bars, which is based on the principle that pitting corrosion causes strain localization of steel bar under tension and DOFS enable to capture the strain distribution with high spatial resolution. DOFS were attached on bare steel bars, which have mechanical notches to simulate corrosion pits, to measure the strain distribution along the notched bars under direct tension. Through experiments, the present study explores the possibility of attaching DOFS on the surface of a steel bar to monitor its pitting corrosion, and the positive results are of interest to the development of non-destructive detection method of steel pitting corrosion in concrete structures. Further quantitative analysis is required to find the correlations between the strain distribution along the notched bars and notch geometries, so that the pitting corrosion level could be assessed from the monitored DOFS strains of rebar.*

**Keywords:** *Pitting Corrosion of Steel Bar, DOFS; Strain Localization, Non-destructive Method.*

## 1 Introduction

Reinforced concrete (RC) is the most widely used building material in the world, and steel rebar corrosion is an important factor that deteriorates the performance of structures. Chloride ion penetration and concrete carbonation are the two major causes of rebar corrosion. The corrosion type of rebar induced by concrete carbonation is usually general corrosion or uniform corrosion, whereas localized pitting corrosion often occurs in RC under the action of chloride penetration, especially at or near the cracking positions of RC structures (Chen et al. 2020a).

Previous studies and practice have shown that only a small depth of uniform corrosion (less than 100 $\mu$ m) would cause longitudinal cracking in concrete cover. The negative side of corrosion-induced cracking is that it can accelerate the corrosion process, while the positive side is that it has been regarded as an indicator of corrosion degree of embedded rebar. In the case of localized pitting corrosion, corrosion cracks may be absent due to the small volume of accumulated corrosion products. However, severe pitting corrosion can seriously decrease both the load and deformation capacities of steel rebar and RC structures (Chen et al. 2020b). Therefore, an efficient and reliable method to detect the pitting corrosion in RC is highly desirable to avoid sudden safety accidents of structures.

It has been reported that traditional corrosion detection methods (such as Linear Polarization Resistance method) based on the electrochemistry principle are unfortunately not accurate in estimating the pitting corrosion rate and level of rebar (Andrade and Alonso, 2004). The present study proposed a new method to detect the pitting corrosion level of steel rebar with the help of distributed optical fiber sensors (DOFS). It has been well known that pitting corrosion can cause strain localization in rebar under tension. DOFS based on Optical Frequency Domain Reflectometer (OFDR) and Rayleigh scattering has high space resolution for strain measurement, which means it can measure the local strain distribution along the rebar in tensile state by a single optical sensor (Berrocal et al. 2021). When the steel bar is equipped with DOFS, the strain peak information detected by DOFS can reflect the pitting corrosion location and degree if the rebar is in tension under external loading.

In this preliminary study, bare steel bars glued with DOFS were tested under uniaxial tension. The strain distributions measured by DOFS were analyzed with respect to the pitting corrosion level of the bars. The types of DOFS and position of DOFS relative to the pit mouth direction were considered in the experiments. In the end, the theoretical strain distribution of a pitting-corroded bar calculated from finite element analysis was compared with the DOFS results.

## 2 Experimental Description

Bare steel bars with elliptical notch simulating corrosion pit were prepared. In total, 15 ribbed bars with the type HRB400-E and 2 smooth bars with the type Q235 were studied. The length of the bars was kept as 500 mm. Three designed notch depths (1.88, 3.05 and 4.08 mm) and three designed notch lengths (10, 20 and 60 mm) were involved. In addition, three ribbed bars respectively had two different notches on them with prescribed distance. Figure 1 and Table 1 show the label of all the bars and their notch geometry. The surface morphology of six bars (i.e. No.1~No.5, No. 16) was scanned by a 3-dimensional scanning equipment ATOS, see Fig. 2. By processing the point cloud data of 3D-scanning, the actual maximum loss of cross-sectional area, defined as the corrosion level in this study, was obtained, also shown in Table 1. It can be seen that the real corrosion level is a little larger than the designed value, which was believed to be caused by the machining error when creating the notch.

The OSI DOFS System made by Wuhan MegaSense Technologies was used in this study. The maximum space resolution is described as 1 mm by the producer. Three types of optical fiber sensors were employed, which included a thin polyimide-coated fiber sensor, a tightly-sheathed fiber sensor and a robust-sheathed fiber sensor (see Fig. 3a). The three types of fiber sensors respectively have 0.125, 0.9 and 2mm in diameter and were denoted as PI-FS, 0.9mm-FS and 2mm-FS in the following. For the ribbed bars, the fiber sensors were deployed along the longitudinal rib(s), see Fig. 3b. In order to compare the results of different types of fiber sensors, different fiber sensor types were glued on the same steel bar. It should be noted that all the notch(es) on the ribbed bars were opened in the region between the two longitudinal ribs, as shown in Fig. 2. For the two smooth bars, the fiber sensors were placed along four lines: one line crossing the notch mouth, one line located at the backside of the notch mouth, and two lines were on the lateral sides of the notch, see Fig. 3c.

The uniaxial tensile tests of steel bars were conducted at a universal testing machine with the load capacity of 100kN. The loading was applied by displacement-controlled mode, with the speed of 0.25mm/min in the initial stage and 5mm/min in the later. The bars were loaded

up to failure. The full load-displacement curves of tested bars were not reported in this paper, as this is not the focus of this study and the DOFS data were only valid when the strain is less than  $12000\mu\epsilon$ .

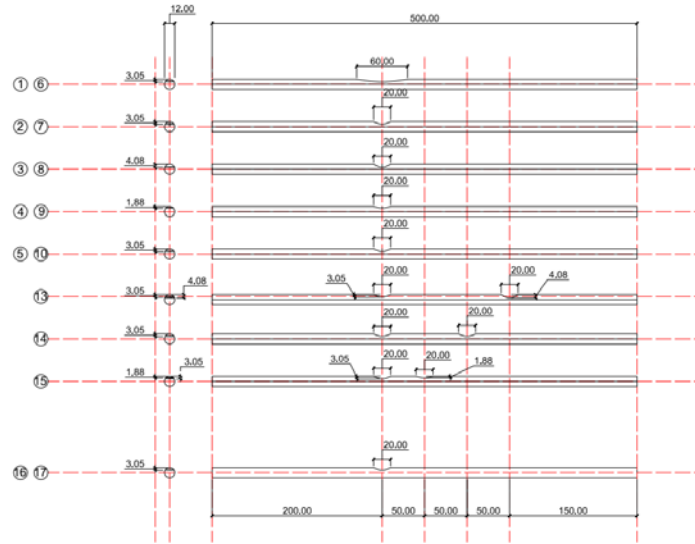


**Figure 1.** Sketch of steel bars with various types of notches.

**Table 1.** Test steel bar parameters.

Bar No.	Steel type	Notch position (mm)	Notch depth (mm)	Notch length (mm)	Designed $\mu_{\max}$ (%)	Measured $\mu_{\max}$ by 3D scanning (%)	Fiber sensors arrangement
1	6	HRB400-E	200	3.05	60	20	24.3
2	7	HRB400-E	200	3.05	20	20	25.1
3	8	HRB400-E	200	4.08	20	30	34.2
4	9	HRB400-E	200	1.88	20	10	17.4
5	10	HRB400-E	200	3.05	10	20	24
11	12	HRB400-E	\	\	\	\	\
13	HRB400-E	200, 350	3.05, 4.08	20, 20	20	25.1	No.1-16 have PI-FS; No.1-5,11-15, and 17 have 0.9mm-FS; No.6-10,13-15 have 2mm-FS.
14	HRB400-E	200, 250	3.05, 1.88	20, 20	20	25.1	
15	HRB400-E	200, 300	3.05, 3.05	20, 20	10	17.4	
					20	25.1	
					20	25.1	
16	17	Q235	200	3.05	20	20	22.4

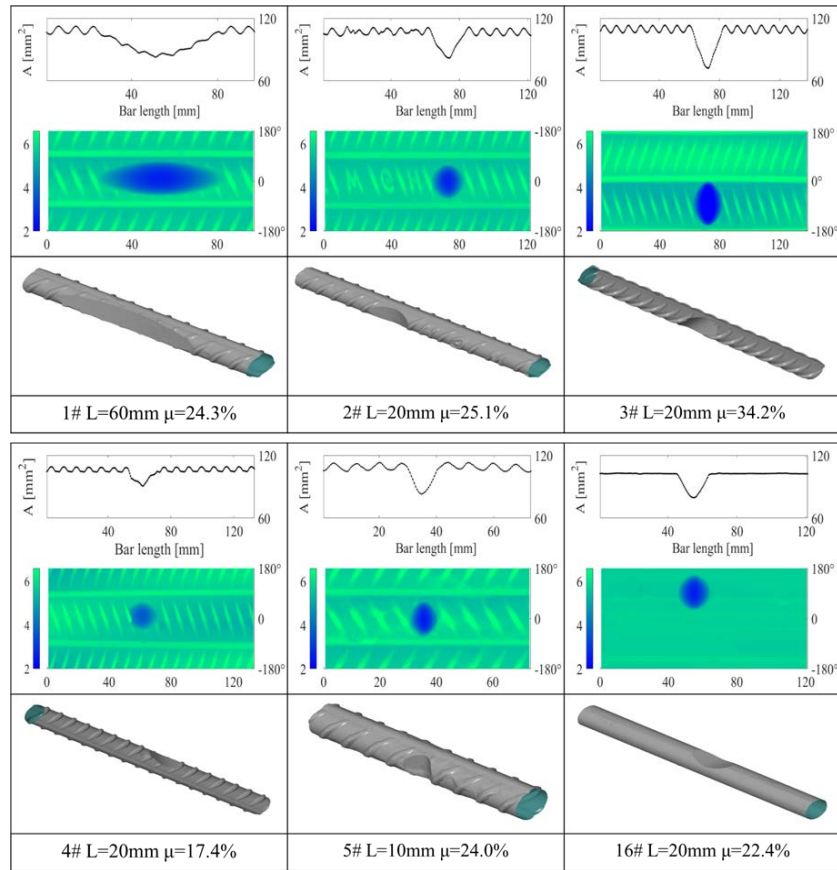


**Figure 2.** 3D-scanning results of six different bars.

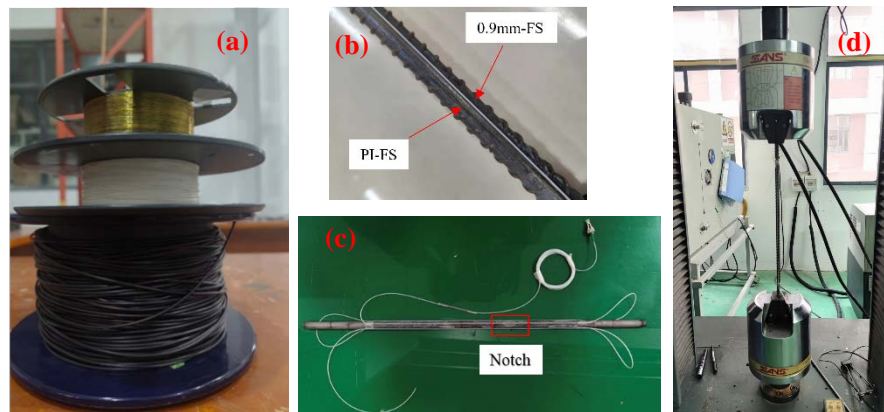


**Figure 3.** (a) Three types of fiber sensors used in this study: PI-FS, 0.9mm-FS and 2mm-FS; (b) Fiber sensors arrangement on ribbed bars; (c) Fiber sensors arrangement on smooth bars; (d) Uniaxial tensile test set-up.

### 3 Experimental Results

This section presents the results of the strain distribution and its evolution of steel bar measured by DOFS with increasing tensile loading. The results from different types of fiber sensors for unnotched and notched bars were first compared to check the accuracy and robustness of

different fiber sensors. Then, the strain evolution of steel bars with different notch forms was examined. Finally, the influence of the DOFS position relative to the notch mouth was studied on the smooth bar.

### 3.1 Strain Distribution of Unnotched Bars Measured by DOFS

The unnotched ribbed bars (i.e. No. 11 and No. 12) were first examined. Figure 4 shows the strain distribution at selected load levels for these two bars. It can be seen that the PI-FS is most sensitive as it can detect the strain changes due to the ribs more clearly than 0.9mm-FS and 2mm-FS. The strain is almost uniform along the bar length except the disturbance caused by the transverse ribs and shear lag effect caused by the glue between sensors and the bar. The Young's modulus of the unnotched steel estimated by the ratio of the stress level to the average strain over a certain length was 191GPa and 194 GPa from PI-FS and 0.9mm-FS results respectively, see Fig. 4. It is close to the value given by the steel producer. This proves that the DOFS can measure the strain accurately.

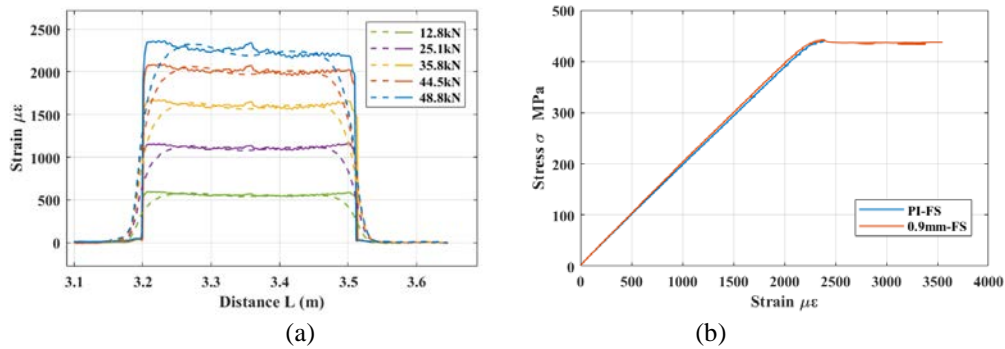


**Figure 4.** (a) Strain distribution measured by PI-FS and 0.9mm-FS for bar No.11; (b) Stress-strain curves from DOFS results.

### 3.2 Strain Distribution of Bars with A Single Notch

From Fig. 5a which compares results of PI-FS and 0.9mm-FS from bar No. 1, it can be seen that PI-FS can detect the strain peak caused by the notch at an earlier stage, whereas 0.9mm-FS is less sensitive. From Fig. 5b which compares results of 0.9mm-FS and 2mm-FS from bar No. 15, it can be seen that these two types of fiber sensors have the more or less same sensitivity and accuracy.

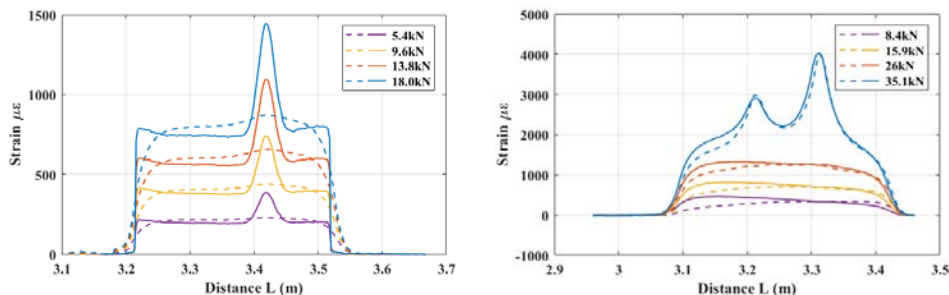


**Figure 5.** (a) Results of PI-FS and 0.9mm-FS from bar No. 1; (b) Results of 0.9mm-FS and 2mm-FS from bar No. 15.

The strain distributions at four selected load levels for ribbed bars with different notch geometries were plotted in Fig. 6. The load levels were kept similar for the different bars for the strain comparison. It can be seen that DOFS can capture the strain localization caused by various notches well. When the notch is kept the same, a deeper notch causes the strain peak larger, and a longer notch gives a smoother peak than the shorter notch under the same notch depth. Further analysis is required to quantitatively correlate the strain distribution with the notch geometry.

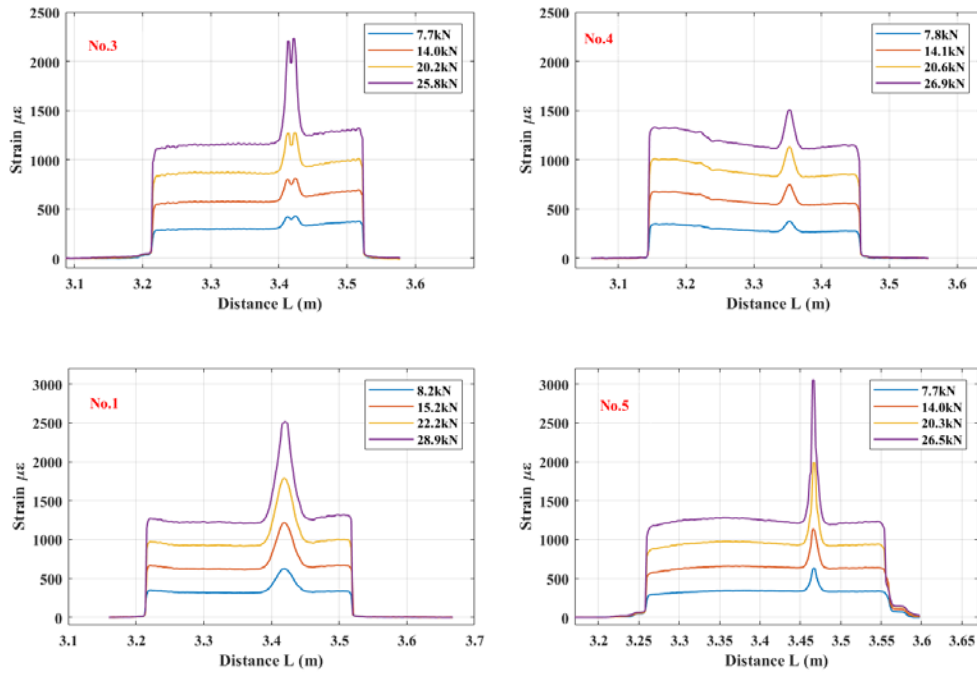


**Figure 6.** Results of bars with different notch geometries measured by PI-FS: bar No. 3 ( $l_p=20\text{mm}$ ,  $x_p=4.08\text{mm}$ ), bar No. 4 ( $l_p=20\text{mm}$ ,  $x_p=1.88\text{mm}$ ), bar No. 1 ( $l_p=60\text{mm}$ ,  $x_p=3.05\text{mm}$ ), and bar No. 5 ( $l_p=10\text{mm}$ ,  $x_p=3.05\text{mm}$ ).

### 3.3 Strain Distribution of the Bar with Two Notches

The bar No. 15 with two same notches at a distance of 100 mm were shown in Fig. 7. It shows that DOFS can capture the two positions of strain localization caused by the two notches well.

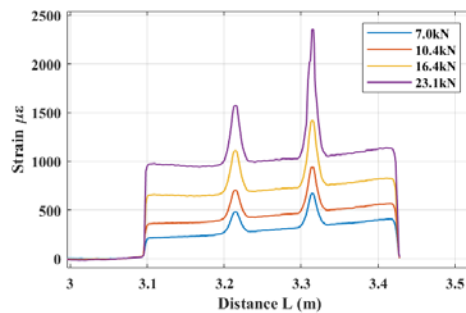


**Figure 7.** Results of bar No. 15 measured by PI-FS.

### 3.4 Strain Distribution of the Smooth Bar

From preliminary quantitative analysis of the above results, it has been found that quantitative relation between the strain peak value and corrosion level of the notch was actually influenced by the relative positive of the fiber sensor to the notch mouth. Since in practice the DOFS may not be located just right at the lateral side of the notch mouth, the influence of DOFS position relative to the notch mouth on the strain distribution was initially studied on a smooth steel bar. From Fig. 8, it can be seen that the region crossed the notch mouth has the highest peak strain. The regions located on the two lateral sides of the notch mouth gave strain peak with less degree. Contrary to the strain peak, the region located on the back of the notch mouth gave a local strain trough. It should be noted that the practical position of DOFS relative to the pit mouth may be arbitrary, and the existence of DOFS may also influence the pitting corrosion development although its size is very small. Therefore, an accurate quantitative evaluation of pitting corrosion level of rebar under tensile state from DOFS strain is still challenging.

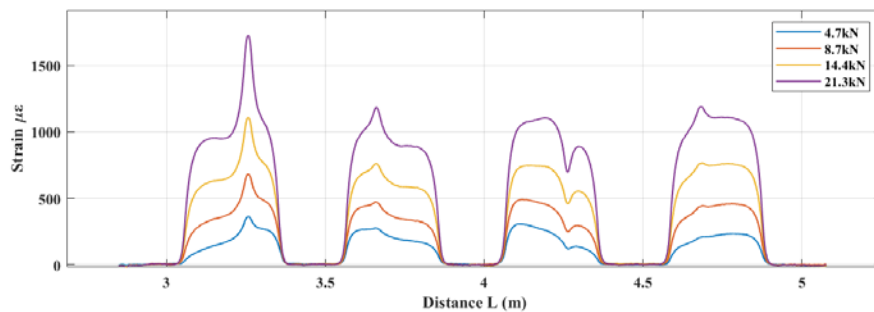


Figure 8. Results of the smooth bar No. 16 measured by 0.9mm-FS.

## 4 Comparison with Finite Element Analysis Results

In order to estimate the pitting corrosion level from the strain distribution monitored by DOFS, the quantitative relationship between the notch geometry and the strain distribution should be investigated. A theoretical derivation may be possible to find this relationship. In this study, a simple numerical analysis on the strain distribution of notched steel bar under tension was carried out with the finite element software Abaqus. The purpose was to compare the strain distributions from DOFS and FE modelling. The finite element model is shown in Fig. 9, and the results comparison is given in Fig. 10. The good agreement suggests that it will be possible to find the notch information by combining the DOFS measurement with the FE analysis.

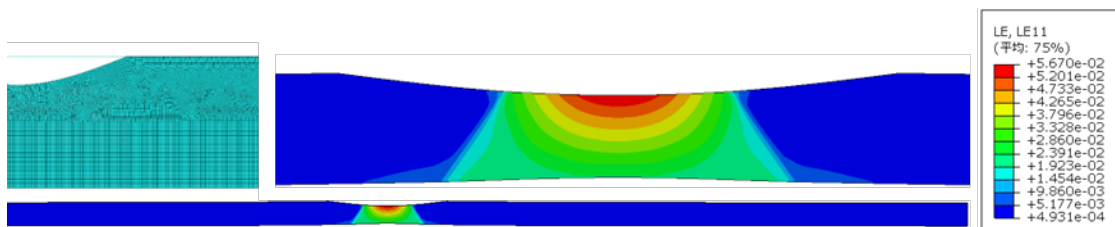
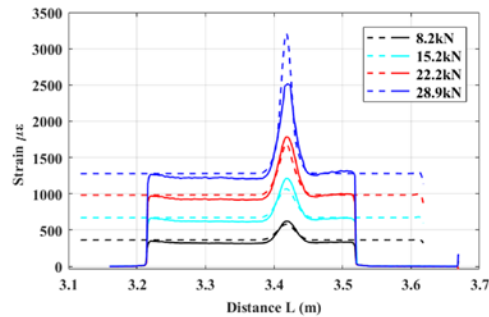


Figure 9. Finite element mesh and strain distribution of notched steel bar under tension.



**Figure 10.** Comparison of strain distributions from FEM (dashed line) and DOFS on bar No. 1 with PI-FS (solid line).

## 5 Conclusion

Through uniaxial tensile tests of notched steel bars, this study explores the ability of DOFS to evaluate the corrosion degree of steel bar with pitting corrosion. The main conclusions are as follows:

- DOFS can monitor the strain localization of notched bars in tension due to its high space resolution. It provides a potential way to detect the pitting corrosion early. However, more quantitative analysis is required to realize the quantitative evaluation of the pitting corrosion level from the strain peak information given by DOFS.
- It was found that the strain distribution of notched steel bar measured by DOFS was significantly affected by the relative position of fiber sensors and notch. Quantitative evaluation of pitting corrosion level by DOFS monitoring should consider this effect.

## References

- Chen E, Berrocal C. G., Löfgren I., Lundgren K. (2020a). *Correlation between concrete cracks and corrosion characteristics of steel reinforcement in pre-cracked plain and fibre-reinforced concrete beams*, Materials and Structures, 53, 33.
- Chen E, Berrocal C. G., Fernandez I., Löfgren I., Lundgren K. (2020b). *Assessment of the mechanical behaviour of reinforcement bars with localised pitting corrosion by Digital Image Correlation*, Engineering Structures, 219, 110936.
- Andrade C, Alonso C (2004). *Test methods for on-site corrosion rate measurement of steel reinforcement in concrete by means of the polarization resistance method*, Materials and Structures, 37, 623–43.
- Berrocal C.G., Fernandez I., Rempling R (2021). *Crack monitoring in reinforced concrete beams by distributed optical fiber sensors*, Structure and Infrastructure Engineering, 17(1), 124-139.